



problem of thermoviscoelasticity for an anisotropic material becomes more important due to its many applications in modern aeronautics, astronautics, earthquake engineering, soil dynamics, nuclear reactors and high-energy particle accelerators. It is hard to find the analytical solution of a problem in a general case, therefore, an important number of engineering and mathematical papers devoted to the numerical solution have studied the overall behavior of such materials (Berezovski and Maugin[6], Misra et al. [7], El-Naggar et al. [8, 9], Abd-Alla et al. [10-12], Fahmy [13-17], Fahmy and El-Shahat [18], Yan and Liu [19]).

Functionally graded materials (FGMs) are a type of nonhomogeneous composites usually made from a mixture of metals and ceramics. FGMs are now developed for general use as structure components in ultrahigh temperature environments and extremely large thermal gradients such as aircraft, space vehicles, automobile industries, nuclear plants and other engineering applications. For a functionally graded (FG) thick strip the material properties are generally assumed to vary continuously in the thickness direction only. The response of an FG thick strip to mechanical and thermal loads may be computed analytically, numerically, or experimentally. We are not aware of experimental results on FG thick strips subjected to transient thermal, magnetic and mechanical loads. And it is well known that the thermal stress distributions in a transient state can show large values compared with the one in a steady state. Therefore, the transient thermoelastic problems for these nonhomogeneous materials become important, and there are several studies concerned with these problems such as Shariyat et al. [20], Afsar and Go [21], Zhang and Batra [22], Arani et al. [23], Khosravifard et al. [24], Rangelov et al. [25], Zhou et al. [26] and Fahmy [27, 28].

One of the most frequently used techniques for converting the domain integral into a boundary one is the so-called dual reciprocity boundary element method (DRBEM). This method was initially developed by Nardini and Brebbia [29] in the context of two-dimensional (2D) elastodynamics and has been extended to deal with a variety of problems wherein the domain integral may account for linear-nonlinear static-dynamic effects. The DRBEM has been highly successful in a very wide range of engineering applications, including acoustics, aeroacoustics, aerodynamics, fluid dynamics, fracture analysis, geomechanics, elasticity and heat transfer. A more extensive historical review and applications of dual reciprocity boundary element method may be found in Brebbia et al. [30], Wrobel and Brebbia [31], Partridge et al. [32], Partridge and Wrobel [33] and Fahmy [34-39] who studied DRBEM problems considering viscoelastic solid of Kelvin-Voigt type.

The present work deals with a two dimensional generalized magneto-thermo-viscoelastic problem for a rotating functionally graded anisotropic thick strip. The problem has been solved using generalized thermoelasticity theory proposed by Green and Naghdi [4]. A predictor-corrector implicit-implicit staggered algorithm was developed and implemented for using with the DRBEM to obtain the solution for the displacement and temperature fields. The transient temperature, and displacement components have been computed numerically and illustrated graphically in the context of the Green and Naghdi theory of type III. It can also be seen from these figures that the effect of rotation is very pronounced. Numerical results that demonstrate the validity of the proposed method are also presented graphically.

## 2. Formulation of the Problem

Consider a Cartesian coordinates system  $Oxyz$  as shown in Fig. 1. We shall consider a functionally graded anisotropic viscoelastic thick strip of a finite thickness  $h$  placed in a primary magnetic field  $H_0$  acting in the direction of the  $z$ -axis and rotating about it with a constant angular velocity in the presence of spatially varying heat source. The strip occupies the region  $R = \{(x, y, z): 0 < x < \underline{\gamma}, 0 < y < \underline{\beta}, 0 < z < \underline{\alpha}\}$  with varying material properties in the thickness direction. Here we address the generalized two-dimensional deformation problem in  $xy$ -plane only; therefore, all the variables are constant along the  $z$ -axis.

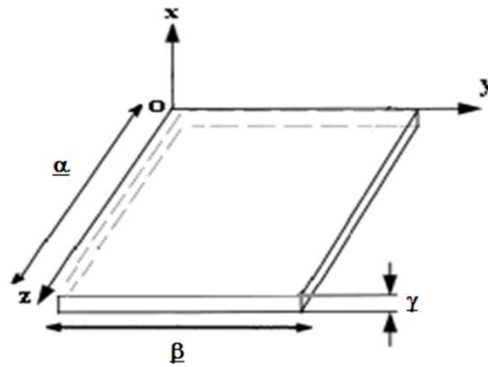


Fig. 1 The coordinate system of the strip

The generalized magneto-thermo-visco-elastic governing differential equations in the context of the Green and Naghdi theory of type III for a Kelvin-Voigt type can be written as

$$\sigma_{ab,b} + E_{ab,b} - \rho' \Omega^2 x_a = \rho' \ddot{u}_a \quad (1)$$

$$\sigma_{ab} = \varkappa [C'_{abfg} u_{f,g} - \beta'_{ab} (T - T_0 + \tau_1 \dot{T})], \varkappa = \left(1 + \nu_0 \frac{\partial}{\partial \tau}\right) (C'_{abfg} = C'_{fgab} = C'_{bafg}), (\beta'_{ab} = \beta'_{ba}) \quad (2)$$

$$E_{ab} = \mu' (\tilde{h}_a H_b + \tilde{h}_b H_a - \delta_{ba} (\tilde{h}_f H_f)), \tilde{h}_a = (\nabla \times (\mathbf{u} \times \mathbf{H}))_a \quad (3)$$

$$\left[ k'_{ab} + k'_{ab} \frac{\partial}{\partial \tau} \right] T_{,ab} + \rho' \dot{\tilde{x}} = \rho' c' \dot{T} + \beta'_{ab} T_0 \ddot{u}_{a,b}, (k'_{ab} = k'_{ba}), (k'_{12})^2 - k'_{11} k'_{22} < 0 \quad (4)$$

The initial and boundary conditions for the current problem are assumed to be written as

$$u_f(x, y, 0) = \dot{u}_f(x, y, 0) = 0 \text{ for } (x, y) \in R \cup C \quad (5)$$

$$u_f(x, y, \tau) = \Psi_f(x, y, \tau) \text{ for } (x, y) \in C_3 \quad (6)$$

$$\bar{t}_a(x, y, \tau) = Y_f(x, y, \tau) \text{ for } (x, y) \in C_4, \tau > 0, C = C_3 \cup C_4, C_3 \cap C_4 = \emptyset \quad (7)$$

$$T(x, y, 0) = \dot{T}(x, y, 0) = 0 \text{ for } (x, y) \in R \cup C \quad (8)$$

$$T(x, y, \tau) = f(x, y, \tau) \text{ for } (x, y) \in C_1, \tau > 0 \quad (9)$$

$$q(x, y, \tau) = \bar{h}(x, y, \tau) \text{ for } (x, y) \in C_2, \tau > 0, C = C_1 \cup C_2, C_1 \cap C_2 = \emptyset \quad (10)$$

A superposed dot denotes differentiation with respect to the time and a comma followed by a subscript denotes partial differentiation with respect to the corresponding coordinates.

For functionally graded materials, the parameters  $C'_{abfg}$ ,  $\beta'_{ab}$ ,  $\mu'$ ,  $\rho'$  and  $k'_{ab}$  are space dependent. In this paper, we have focused our attention on studying the effect of inhomogeneity along the  $0x$  direction. Thus, we replace these quantities by  $C_{abfg}f(x)$ ,  $\beta_{ab}f(x)$ ,  $\mu f(x)$ ,  $\rho f(x)$  and  $k_{ab}f(x)$  where  $C_{abfg}$ ,  $\beta_{ab}$ ,  $\mu$ ,  $\rho$  and  $k_{ab}$  are assumed to be constants and  $f(x)$  is a given nondimensional function of space variable  $x$ . We take  $f(x) = (x + 1)^m$ , where  $m$  is a dimensionless constant. Then the equations (1)-(4) become

$$\sigma_{ab,b} + \tau_{ab,b} - \rho(x+1)^m \Omega^2 x_a = \rho(x+1)^m \ddot{u}_a \quad (11)$$

$$\sigma_{ab} = \varkappa(x+1)^m [C_{abfg} u_{f,g} - \beta_{ab}(T - T_0 + \tau_1 \dot{T})] \quad (12)$$

$$\tau_{ab} = \mu(x+1)^m (\tilde{h}_a H_b + \tilde{h}_b H_a - \delta_{ba}(\tilde{h}_f H_f)) \quad (13)$$

$$\left[ k_{ab}^* + k_{ab} \frac{\partial}{\partial \tau} \right] T_{,ab} + \rho \dot{\varkappa} = \rho c(x+1)^m \dot{T} + \beta_{ab} T_0 \ddot{u}_{a,b} \quad (14)$$

### 3. Numerical Implementation

Making use of Eqs. (12) and (13), we can write (11) as follows

$$L_{gb} u_f = \rho \ddot{u}_a - (D_a T - \rho \Omega^2 x_a) = f_{gb} \quad (15)$$

where the inertia term  $\rho \ddot{u}_a$ , the temperature gradient  $D_a T$  and rotation term  $\rho \Omega^2 x_a$  are treated as the body forces. The field equations can now be written in operator form as follows

$$L_{gb} u_f = f_{gb} \quad (16)$$

$$L_{ab} T = f_{ab} \quad (17)$$

where the operators  $L_{gb}$ ,  $f_{gb}$ ,  $L_{ab}$  and  $f_{ab}$  are defined as follows:

$$L_{gb} = D_{abf} \frac{\partial}{\partial x_b} + D_{af} + \Lambda D_{a1f}, f_{gb} = \rho \ddot{u}_a - D_a T + \rho \Omega^2 x_a \quad (18)$$

$$L_{ab} = k_{ab}^* \frac{\partial}{\partial x_a} \frac{\partial}{\partial x_b}, f_{ab} = k_{ab} \dot{T}_{,ab} + \rho c(x+1)^m \dot{T} + \beta_{ab} T_0 \ddot{u}_{a,b} - \rho \dot{\varkappa} \quad (19)$$

Where

$$D_{abf} = C_{abfg} \varkappa \varepsilon, \quad \varepsilon = \frac{\partial}{\partial x_g}, \quad D_{af} = \mu H_0^2 \left( \frac{\partial}{\partial x_a} + \delta_{a1} \Lambda \right) \frac{\partial}{\partial x_f},$$

$$D_a = -\beta_{ab} \left( \frac{\partial}{\partial x_b} + \delta_{b1} \Lambda + \tau_1 \left( \frac{\partial}{\partial x_b} + \Lambda \right) \frac{\partial}{\partial \tau} \right), \quad \Lambda = \frac{m}{x+1}$$

Using the weighted residual method (WRM), the differential equation (16) is transformed into an integral equation

$$\int_R (L_{gb} u_f - f_{gb}) u_{da}^* dR = 0 \quad (20)$$

Now, we choose the fundamental solution  $u_{df}^*$  defined by

$$L_{gb} u_{df}^* = -\delta_{ad} \delta(x, \xi) \quad (21)$$

as weighting function

The corresponding traction field can be written as

$$t_{da}^* = C_{abfg} \aleph u_{df,g}^* n_b \quad (22)$$

The thermoelastic traction vector can be written as follows

$$t_a = \frac{\bar{t}_a}{(x+1)^m} = (C_{abfg} \aleph u_{f,g} - \beta_{ab}(T + \tau_1 \dot{T})) n_b \quad (23)$$

Applying integration by parts to (20) using the sifting property of the Dirac distribution, with (22) and (23), we can write the following elastic integral representation formula

$$u_d(\xi) = \int_C (u_{da}^* t_a - t_{da}^* u_a + u_{da}^* \beta_{ab} T n_b) dC - \int_R f_{gb} u_{da}^* dR \quad (24)$$

The fundamental solution  $T^*$  of the thermal operator  $L_{ab}$  is described mathematically by the Dirac distribution  $\delta(x, \xi)$  as follows

$$L_{ab} T^* = -\delta(x, \xi) \quad (25)$$

where  $x$  is the field point and  $\xi$  is the load point; By implementing the WRM and integration by parts, the differential equation (17) is transformed into the thermal reciprocity equation

$$\int_R (L_{ab} T T^* - L_{ab} T^* T) dR = \int_C (q^* T - q T^*) dC \quad (26)$$

where the heat fluxes are independent of the elastic field and can be expressed as follows:

$$q = -k_{ab} T_{,b} n_a \quad (27)$$

$$q^* = -k_{ab} T^*_{,b} n_a \quad (28)$$

By the use of sifting property, we obtain from (26) the thermal integral representation formula

$$T(\xi) = \int_C (q^* T - q T^*) dC - \int_R f_{ab} T^* dR \quad (29)$$

The integral representation formulae of elastic and thermal fields (24) and (29) can be combined to form a single equation as follows

$$\begin{bmatrix} u_d(\xi) \\ T(\xi) \end{bmatrix} = \int_C \left\{ - \begin{bmatrix} t_{da}^* & -u_{da}^* \beta_{ab} n_b \\ 0 & -q^* \end{bmatrix} \begin{bmatrix} u_a \\ T \end{bmatrix} + \begin{bmatrix} u_{da}^* & 0 \\ 0 & -T^* \end{bmatrix} \begin{bmatrix} t_a \\ q \end{bmatrix} \right\} dC - \int_R \begin{bmatrix} u_{da}^* & 0 \\ 0 & -T^* \end{bmatrix} \begin{bmatrix} f_{gb} \\ -f_{ab} \end{bmatrix} dR \quad (30)$$

It is convenient to use the contracted notation to introduce generalized thermoelastic vectors and tensors, which contain corresponding elastic and thermal variables as follows:

$$U_A = \begin{cases} u_a & a = A = 1, 2, 3 \\ T & A = 4 \end{cases} \quad (31)$$

$$T_A = \begin{cases} t_a & a = A = 1, 2, 3 \\ q & A = 4 \end{cases} \quad (32)$$

$$U_{DA}^* = \begin{cases} u_{da}^* & d = D = 1, 2, 3; a = A = 1, 2, 3 \\ 0 & d = D = 1, 2, 3; A = 4 \\ 0 & D = 4; a = A = 1, 2, 3 \\ -T^* & D = 4; A = 4 \end{cases} \quad (33)$$

$$\tilde{T}_{DA}^* = \begin{cases} t_{da}^* & d = D = 1, 2, 3; a = A = 1, 2, 3 \\ -\tilde{u}_d^* & d = D = 1, 2, 3; A = 4 \\ 0 & D = 4; a = A = 1, 2, 3 \\ -q^* & D = 4; A = 4 \end{cases} \quad (34)$$

$$\tilde{u}_d^* = u_{da}^* \beta_{af} n_f \quad (35)$$

Using the contracted notation, the thermoelastic representation formula (30) can be written as:

$$U_D(\xi) = \int_C (U_{DA}^* T_A - \tilde{T}_{DA}^* U_A) dC - \int_R U_{DA}^* S_A dR \quad (36)$$

The vector  $S_A$  can be written in the split form as follows

$$S_A = S_A^0 + S_A^T + S_A^{\dot{T}} + S_A^{\ddot{T}} + S_A^{\ddot{u}} \quad (37)$$

Where

$$S_A^0 = \begin{cases} \rho \Omega^2 x_a & A = 1, 2, 3 \\ \rho \dot{x} & A = 4 \end{cases} \quad (38)$$

$$S_A^T = \omega_{AF} U_F \text{ wit } \omega_{AF} = \begin{cases} -D_a & A = 1, 2, 3; F = 4 \\ 0 & \end{cases} \quad (39)$$

$$S_A^{\dot{T}} = \Gamma_{AF} \dot{U}_F \text{ wit } \Gamma_{AF} = \begin{cases} -k_{ab} \frac{\partial}{\partial x_a} \frac{\partial}{\partial x_b} & A = 4; F = 4 \\ 0 & \end{cases} \quad (40)$$

$$S_A^{\ddot{T}} = \delta_{AF} \ddot{U}_F \text{ wit } \delta_{AF} = \begin{cases} -c\rho(x+1)^m & A = 4; F = 4 \\ 0 & \text{ot erwise} \end{cases} \quad (41)$$

$$S_A^{\ddot{u}} = \mathfrak{d} \ddot{U}_F \text{ with } \mathfrak{d} = \begin{cases} \rho & A = 1, 2, 3; F = 1, 2, 3 \\ -T_0 \beta_{fg} \varepsilon & A = 4; F = 4 \end{cases} \quad (42)$$

The thermoelastic representation formula (30) can also be written in matrix form as follows:

$$[S_A] = \begin{bmatrix} \rho \Omega^2 x_a \\ \rho \dot{x} \end{bmatrix} + \begin{bmatrix} -D_a T \\ 0 \end{bmatrix} + \begin{bmatrix} 0 \\ -k_{ab} \dot{T}_{,ab} \end{bmatrix} - \rho c (x+1)^m \begin{bmatrix} 0 \\ \ddot{T} \end{bmatrix} + \begin{bmatrix} \rho \ddot{u}_a \\ -\beta_{fg} T_0 \ddot{u}_{f,g} \end{bmatrix} \quad (43)$$

Our task now is to implement the DRBEM. To transform the domain integral in (36) to the boundary, we approximate the source vector  $S_A$  in the domain as usual by a series of given tensor functions  $f_{AE}^q$  and unknown coefficients  $\alpha_E^q$

$$S_A \approx \sum_{q=1}^E f_{AE}^q \alpha_E^q \quad (44)$$

Thus, the thermoelastic representation formula (36) can be written in the following form

$$U_D(\xi) = \int_C (U_{DA}^* T_A - \tilde{T}_{DA}^* U_A) dC - \sum_{q=1}^N \int_R U_{DA}^* f_{AE}^q dR \alpha_E^q \quad (45)$$

By applying the WRM to the following inhomogeneous elastic and thermal equations:

$$L_{gb} u_{fe}^q = f_{ae}^q \quad (46)$$

$$L_{ab} T^q = f_{pj}^q \quad (47)$$

where the weighting functions are chosen to be the elastic and thermal fundamental solutions  $u_{da}^*$  and  $T^*$ . Then the elastic and thermal representation formulae are similar to those of Fahmy [40] within the context of the uncoupled theory and are given as follows

$$u_{de}^q(\xi) = \int_C (u_{da}^* t_{ae}^q - t_{da}^* u_{ae}^q) dC - \int_R u_{da}^* f_{ae}^q dR \quad (48)$$

$$T^q(\xi) = \int_C (q^* T^q - q^q T^*) dC - \int_R f^q T^* dR \quad (49)$$

The dual representation formulae of elastic and thermal fields can be combined to form a single equation as follows

$$U_{DE}^q(\xi) = \int_C (U_{DA}^* T_{AE}^q - T_{DA}^* U_{AE}^q) dC - \int_R U_{DA}^* f_{AE}^q dR \quad (50)$$

with the substitution of (50) into (45), the dual reciprocity representation formula of coupled thermoelasticity can be expressed as follows

$$U_D(\xi) = \int_C (U_{DA}^* T_A - \tilde{T}_{DA}^* U_A) dC + \sum_{q=1}^E \left( U_{DE}^q(\xi) + \int_C (T_{DA}^* U_{AE}^q - U_{DA}^* T_{AE}^q) dC \right) \alpha_E^q \quad (51)$$

To calculate interior stresses, (54) is differentiated with respect to  $\xi_l$  as follows

$$\frac{\partial U_D(\xi)}{\partial \xi_l} = - \int_C (U_{DA,l}^* T_A - \tilde{T}_{DA,l}^* U_A) dC + \sum_{q=1}^E \left( \frac{\partial U_{DE}^q(\xi)}{\partial \xi_l} - \int_C (T_{DA,l}^* U_{AE}^q - U_{DA,l}^* T_{AE}^q) dC \right) \alpha_E^q \quad (52)$$

According to the steps described in Fahmy [41], the dual reciprocity boundary integral equation (51) can be written in the following system of equations

$$\zeta U - \eta T = (\zeta \check{U} - \eta \check{\phi}) \alpha \tag{53}$$

Where  $\zeta$  contains the fundamental solution  $T_M^*$  and  $\check{\zeta}$  contains the modified fundamental tensor  $\check{T}_M^*$  with the coupling term. The technique which was proposed by Partridge et al. [32] can be extended to treat the convective terms, then the generalized displacements  $U_F$  are approximated by a series of tensor functions  $f_{FD}^q$  and unknown coefficients  $\gamma_D^q$

$$U_F \approx \sum_{q=1}^N f_{FD}^q(x) \gamma_D^q \tag{54}$$

where

$$f_{FD}^q = \begin{cases} f_{fd}^q & f = F = 1,2,3; d = D = 1,2,3 \\ f^q & F = 4; D = 4 \\ 0 & \text{Otherwise} \end{cases} \tag{55}$$

The gradients of the generalized displacement can be approximated with the derivatives of tensor functions as follows

$$U_{F,g} \approx \sum_{q=1}^N f_{FD,g}^q(x) \gamma_D^q \tag{56}$$

These approximations are substituted into Eq. (39) to approximate the corresponding source terms as follows

$$S_A^T = \sum_{q=1}^N S_{AF} f_{FD,g}^q \gamma_D^q \tag{57}$$

The same point collocation procedure described in Gaul et al. [42] can be applied to (44) and (54). This leads to the following system of equations

$$\check{S} = J \alpha, U = J' \gamma \tag{58}$$

Similarly, the application of the point collocation procedure to the source terms equations (57), (40), (41) and (42) leads to the following system of equations

$$\check{S}^T = B^T \gamma \tag{59}$$

$$\check{S}^T = \bar{\Gamma}_{AF} \dot{U} \tag{60}$$

$$\check{S}^T = \bar{\delta}_{AF} \dot{U} \tag{61}$$

$$\check{S}^{\ddot{u}} = \bar{\Xi} \ddot{U} \tag{62}$$

Where  $\bar{\Gamma}_{AF}$ ,  $\bar{\delta}_{AF}$  and  $\bar{\Xi}$  are assembled by using the submatrices  $[\Gamma_{AF}]$ ,  $[\delta_{AF}]$  and  $[d]$  respectively.



Solving the system (58) for  $\alpha$  and yields

$$\alpha = J^{-1}\check{S}, \gamma = J'^{-1}U \quad (63)$$

Now, the coefficients  $\alpha$  can be expressed in terms of nodal values of the unknown displacements  $\check{U}$ , velocities  $\check{U}$  and accelerations  $\check{U}$  as follows:

$$\alpha = J^{-1}(\check{S}^0 + \mathcal{B}^T J'^{-1}U + \bar{\Gamma}_{AF}\check{U} + (\bar{\mathfrak{A}} + \bar{\delta}_{AF})\check{U}) \quad (64)$$

An implicit-implicit staggered algorithm of Farhat et al. [43] was developed and implemented for use with the DRBEM for solving the governing equations which may now be written in a more convenient form after substitution of Eq. (64) into Eq. (53) as follows:

$$\hat{M}\check{U} + \hat{\Gamma}\check{U} + \hat{K}U = \hat{Q} \quad (65)$$

$$\hat{X}\check{T} + \hat{A}\check{T} + \hat{B}T = \hat{Z}\check{U} + \hat{R} \quad (66)$$

Where

$$V = (\zeta\check{U} - \eta\check{\rho})J^{-1}, \quad \hat{M} = V(\bar{\mathfrak{A}} + \bar{\delta}_{AF}), \quad \hat{\Gamma} = V\bar{\Gamma}_{AF},$$

$$\hat{K} = -\zeta + V\mathcal{B}^T J'^{-1}, \quad \hat{Q} = -\eta\check{T} + V\check{S}^0, \quad \hat{X} = -\rho c(x+1)^m,$$

$$\hat{A} = k_{ab} \frac{\partial}{\partial x_a} \frac{\partial}{\partial x_b}, \quad \hat{B} = k_{ab}^* \frac{\partial}{\partial x_a} \frac{\partial}{\partial x_b}, \quad \hat{Z} = \beta_{ab} T_0,$$

$$\hat{R} = -\rho\check{x}$$

where  $V$ ,  $\hat{M}$ ,  $\hat{\Gamma}$  and  $\hat{K}$  represent the volume, mass, damping and stiffness matrices, respectively,  $\check{U}$ ,  $\check{U}$ ,  $U$ ,  $T$  and  $\hat{Q}$  represent the acceleration, velocity, displacement, temperature and external force vectors, respectively,  $\hat{A}$  and  $\hat{B}$  are respectively the capacity and conductivity matrices,  $\hat{X}$  is a vector of new material constants proposed by Green and Lindsay [3],  $\hat{Q}$ ,  $\hat{Z}$  and  $\hat{R}$  are coupling matrices. Hence, the governing equations lead to the following coupled system of differential-algebraic equations (DAEs) as in Farhat et al. [43]:

$$\hat{M}\check{U}_{n+1} + \hat{\Gamma}\check{U}_{n+1} + \hat{K}U_{n+1} = \hat{Q}_{n+1}^p \quad (67)$$

$$\hat{X}\check{T}_{n+1} + \hat{A}\check{T}_{n+1} + \hat{B}T_{n+1} = \hat{Z}\check{U}_{n+1} + \hat{R} \quad (68)$$

where  $\hat{Q}_{n+1}^p = -\eta T_{n+1}^p + V\check{S}^0$  and  $T_{n+1}^p$  is the predicted temperature. Integrating Eq. (65) with the use of trapezoidal rule and Eq. (67), we obtain

$$\begin{aligned} \check{U}_{n+1} &= \check{U}_n + \frac{\Delta\tau}{2}(\check{U}_{n+1} + \check{U}_n) \\ &= \check{U}_n + \frac{\Delta\tau}{2} \left[ \check{U}_n + \hat{M}^{-1} (\hat{Q}_{n+1}^p - \hat{\Gamma}\check{U}_{n+1} - \hat{K}U_{n+1}) \right] \end{aligned} \quad (69)$$

$$\begin{aligned}
 U_{n+1} &= U_n + \frac{\Delta\tau}{2}(\dot{U}_{n+1} + \dot{U}_n) \\
 &= U_n + \Delta\tau\dot{U}_n + \frac{\Delta\tau^2}{4}\left[\dot{U}_n + \tilde{M}^{-1}\left(\tilde{Q}_{n+1}^p - \tilde{F}\dot{U}_{n+1} - \tilde{K}U_{n+1}\right)\right]
 \end{aligned} \tag{70}$$

From Eq. (69) we have

$$\dot{U}_{n+1} = \bar{Y}^{-1}\left[\dot{U}_n + \frac{\Delta\tau}{2}\left[\dot{U}_n + \tilde{M}^{-1}\left(\tilde{Q}_{n+1}^p - \tilde{K}U_{n+1}\right)\right]\right], \quad \bar{Y} = \left(I + \frac{\Delta\tau}{2}\tilde{M}^{-1}\tilde{F}\right) \tag{71}$$

Substituting from Eq. (71) into Eq. (70), we derive

$$\begin{aligned}
 U_{n+1} &= U_n + \Delta\tau\dot{U}_n \\
 &+ \frac{\Delta\tau^2}{4}\left[\dot{U}_n + \tilde{M}^{-1}\left(\tilde{Q}_{n+1}^p - \tilde{F}\bar{Y}^{-1}\left[\dot{U}_n + \frac{\Delta\tau}{2}\left[\dot{U}_n + \tilde{M}^{-1}\left(\tilde{Q}_{n+1}^p - \tilde{K}U_{n+1}\right)\right]\right] - \tilde{K}U_{n+1}\right)\right]
 \end{aligned} \tag{72}$$

Substituting  $\dot{U}_{n+1}^i$  from Eq. (71) into Eq. (67) we obtain

$$\dot{U}_{n+1} = \tilde{M}^{-1}\left[\tilde{Q}_{n+1}^p - \tilde{F}\left[\bar{Y}^{-1}\left[\dot{U}_n + \frac{\Delta\tau}{2}\left[\dot{U}_n + \tilde{M}^{-1}\left(\tilde{Q}_{n+1}^p - \tilde{K}U_{n+1}\right)\right]\right]\right] - \tilde{K}U_{n+1}\right] \tag{73}$$

Integrating the heat equation (66) using the trapezoidal rule, and Eq. (68) we get

$$\begin{aligned}
 \dot{T}_{n+1} &= \dot{T}_n + \frac{\Delta\tau}{2}(\ddot{T}_{n+1} + \ddot{T}_n) \\
 &= \dot{T}_n + \frac{\Delta\tau}{2}\left(\tilde{X}^{-1}\left[\tilde{Z}\dot{U}_{n+1} + \tilde{R} - \tilde{A}\dot{T}_{n+1} - \tilde{B}T_{n+1}\right] + \ddot{T}_n\right)
 \end{aligned} \tag{74}$$

$$\begin{aligned}
 T_{n+1} &= T_n + \frac{\Delta\tau}{2}(\dot{T}_{n+1} + \dot{T}_n) \\
 &= T_n + \Delta\tau\dot{T}_n + \frac{\Delta\tau^2}{4}\left(\dot{T}_n + \tilde{X}^{-1}\left[\tilde{Z}\dot{U}_{n+1} + \tilde{R} - \tilde{A}\dot{T}_{n+1} - \tilde{B}T_{n+1}\right]\right)
 \end{aligned} \tag{75}$$

From Eq. (74) we get

$$\dot{T}_{n+1} = Y^{-1}\left[\dot{T}_n + \frac{\Delta\tau}{2}\left(\tilde{X}^{-1}\left[\tilde{Z}\dot{U}_{n+1} + \tilde{R} - \tilde{B}T_{n+1}\right] + \ddot{T}_n\right)\right], \quad Y = \left(I + \frac{1}{2}\tilde{A}\Delta\tau\tilde{X}^{-1}\right) \tag{76}$$

Substituting from Eq. (76) into Eq. (75), we have

$$\begin{aligned}
 T_{n+1} &= T_n + \Delta\tau\dot{T}_n + \frac{\Delta\tau^2}{4}\left(\dot{T}_n + \tilde{X}^{-1}\left[\tilde{Z}\dot{U}_{n+1} + \tilde{R} \right. \right. \\
 &\left. \left. - \tilde{A}\left(Y^{-1}\left[\dot{T}_n + \frac{\Delta\tau}{2}\left(\tilde{X}^{-1}\left[\tilde{Z}\dot{U}_{n+1} + \tilde{R} - \tilde{B}T_{n+1}\right] + \ddot{T}_n\right)\right]\right) - \tilde{B}T_{n+1}\right]\right)
 \end{aligned} \tag{77}$$

Substituting  $\hat{T}_{n+1}^i$  from Eq. (76) into Eq. (68) we obtain

$$\begin{aligned} \ddot{T}_{n+1} &= \hat{X}^{-1} \left[ \hat{Z} \ddot{U}_{n+1} + \hat{R} \right. \\ &\left. - \hat{A} \left( Y^{-1} \left[ \dot{T}_n + \frac{\Delta\tau}{2} \left( \hat{X}^{-1} \left[ \hat{Z} \dot{U}_{n+1} + \hat{R} - \hat{B} T_{n+1} \right] + \ddot{T}_n \right) \right] \right) - \hat{B} T_{n+1} \right] \end{aligned} \quad (78)$$

Now, a displacement predicted staggered procedure for the solution of (72) and (77) is:

- (1) Predict the displacement field:  $U_{n+1}^p = U_n$
- (2) Substituting for  $\dot{U}_{n+1}$  and  $\ddot{U}_{n+1}$  from equations (69) and (67) respectively in Eq. (77) and solve the resulted equation for the temperature field
- (3) Correct the displacement field using the computed temperature field for the Eq. (72)
- (4) Compute  $\dot{U}_{n+1}$ ,  $\ddot{U}_{n+1}$ ,  $\dot{T}_{n+1}$  and  $\ddot{T}_{n+1}$  from Eqs. (71), (73), (74) and (78) respectively

#### 4. Numerical Results and Discussion

Following Fahmy [40] monoclinic graphite-epoxy material is chosen for the purpose of numerical calculations, the physical data for which is given as follows:

Elasticity tensor

$$C_{abfg} = \begin{bmatrix} 430.1 & 130.4 & 18.2 & 0 & 0 & 201.3 \\ 130.4 & 116.7 & 21.0 & 0 & 0 & 70.1 \\ 18.2 & 21.0 & 73.6 & 0 & 0 & 2.4 \\ 0 & 0 & 0 & 19.8 & -8.0 & 0 \\ 0 & 0 & 0 & -8.0 & 29.1 & 0 \\ 201.3 & 70.1 & 2.4 & 0 & 0 & 147.3 \end{bmatrix} \text{ GPa}$$

Mechanical temperature coefficient

$$\beta_{ab} = \begin{bmatrix} 1.01 & 2.00 & 0 \\ 2.00 & 1.48 & 0 \\ 0 & 0 & 7.52 \end{bmatrix} \cdot 10^6 \text{ N/Km}^2$$

Tensor of thermal conductivity is

$$k_{ab} = \begin{bmatrix} 5.2 & 0 & 0 \\ 0 & 7.6 & 0 \\ 0 & 0 & 38.3 \end{bmatrix} \text{ W/km}$$

Mass density  $\rho = 7820 \text{ kg/m}^3$  and heat capacity  $c = 461 \text{ J/(kgK)}$ ,  $H_0 = 1000000 \text{ Oersted}$ ,  $\mu = 0.5 \text{ Gauss/Oersted}$ ,  $\varkappa = 2$ ,  $h = 2$ ,  $\Delta\tau = 0.0001$ ,  $T_0 = 1$ . The numerical values of the temperature and displacement are obtained by discretizing the boundary into 120 elements ( $N_b = 120$ ) and choosing 60 well spaced out collocation points ( $N_i = 60$ ) in the interior of the solution domain, refer to the recent work of Fahmy [41].

The initial and boundary conditions considered in the calculations are

$$\tau = 0 \quad \dot{u}_1 = \dot{u}_2 = \ddot{u}_1 = \ddot{u}_2 = 0, \quad T = T_0 \quad (79)$$

$$x = 0 \quad \frac{\partial u_1}{\partial x} = \frac{\partial u_2}{\partial x} = 0, \quad T = 0 \quad (80)$$

$$x = \underline{\gamma} \quad u_1 = u_2 = 0, \quad \frac{\partial T}{\partial x} = 0 \quad (81)$$

$$y = 0 \quad \frac{\partial u_1}{\partial y} = \frac{\partial u_2}{\partial y} = 0, \quad T = 0 \quad (82)$$

$$y = \underline{\beta} \quad u_1 = u_2 = 0, \quad \frac{\partial T}{\partial y} = 0 \quad (83)$$

The present work should be applicable to any generalized magneto-thermoelastic deformation problem. The application is for the purpose of illustration; we don't intend to validate the results in a quantitative way because we have no experimental data at hand; this may be justified because our objective is to introduce a viable numerical technique for studying a model rather than to study any physical behaviors of it. Such a technique was discussed by Fahmy [41] who solved the special case from this study in the context of the uncoupled problem. To achieve better efficiency than the technique described in Fahmy [41], we use the implicit algebraic augmentation (IAA) procedure proposed by Farhat et al. [43] into a DRBEM code, which is proposed in the current study. In order to evaluate the influence of the rotation on the temperature and displacements in an anisotropic magneto-thermoviscoelastic thick strip, the uniform angular velocity values are taken to be 0.0, 0.5 and 1.0.

Fig. 2 is plotted to show the variation of the temperature  $T$  along the thickness of the thick strip. It is noticed that the temperature increases with the increase of  $x$  in the absence ( $\Omega = 0.0$ ) and presence ( $\Omega = 0.5$  and  $1.0$ ) of rotation. Also, the temperature decreases with increasing angular velocity.

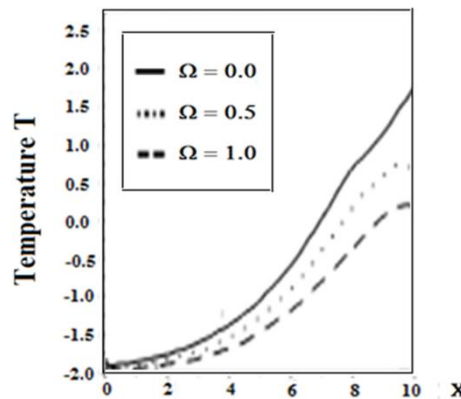


Fig. 2 Variation of the temperature  $T$  along the strip thickness

Fig. 3 and Fig. 4 show the influence of the rotation on the displacements  $u_1$  and  $u_2$  along the strip thickness. It is clear from these figures that the displacement  $u_1$  increases until it reaches its maximum value then it decreases slowly along the thickness of the thick strip for all values of the uniform angular velocity  $\Omega$ , and it decreases with increasing the uniform angular velocity  $\Omega$ . It can also be seen from the figures that the displacement  $u_2$  increases with increasing  $x$  through the thickness of the thick strip and it decreases with the increase of the uniform angular velocity  $\Omega$ .

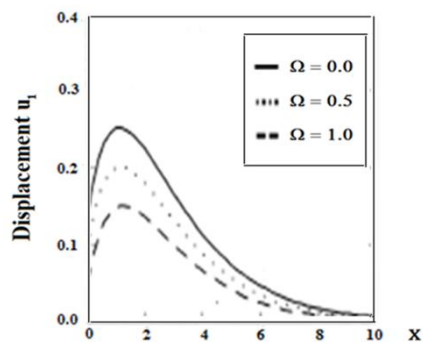


Fig. 3 Variation of the displacement  $u_1$  along the strip thickness

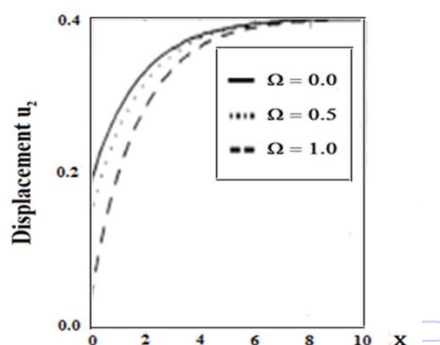


Fig. 4 Variation of the displacement  $u_2$  along the strip thickness

The present work should be applicable to any magneto-thermo-visco-elastic problem in a rotating functionally graded anisotropic thick strip. The example considered by Sladek et al. [44] may be considered as a special case of the current general problem.

In the special case under consideration, the results are plotted in Figs. 5-7 to show the validity of the DRBEM. These results obtained with the DRBEM have been compared graphically with those obtained by using the Meshless Local Petrov-Galerkin (MLPG) method of Sladek et al. [44] and also the results obtained by using the Finite Difference Method (FDM) of Fahmy [45] are shown graphically in the same figures to confirm the validity of the proposed method. It can be seen from these figures that the DRBEM results are in excellent agreement with the results obtained by MLPG and FDM, thus confirming the accuracy of the DRBEM.

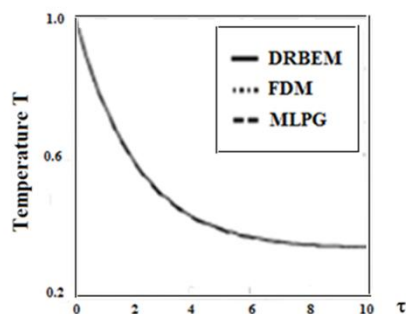


Fig. 5 Variation of the temperature  $T$  with time  $\tau$  for three methods DRBEM, FDM and MLPG

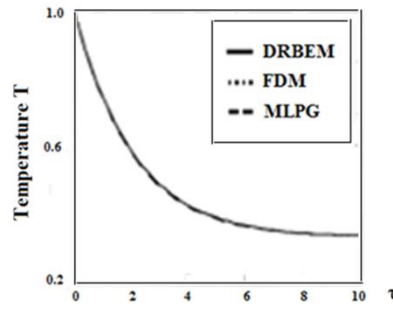


Fig. 6 Variation of the displacement  $u_1$  with time  $\tau$  for three methods DRBEM, FDM and MLPG

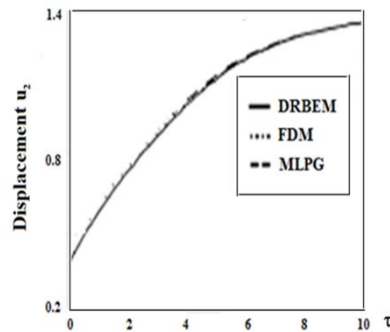


Fig. 7 Variation of the displacement  $u_2$  with time  $\tau$  for three methods DRBEM, FDM and MLPG

From this knowledge of the variation of magneto-thermoviscoelastic displacements in a rotating functionally graded anisotropic strip along its thickness, we can design various magneto-visco-elastic FG strips under thermal load to meet specific engineering requirements and utilize it in measurement techniques of magneto-thermoviscoelasticity.

### Nomenclature

$u_k$	components of displacement	$\tau$	time
$T$	temperature	$\tilde{h}$	perturbed magnetic field
$c'$	specific heat capacity	$H$	magnetic intensity vector
$\mu'$	magnetic permeability	$\rho'$	density
$\mathfrak{X}$	heat source	$C'_{abfg}$	constant elastic moduli
$\mathfrak{N}$	viscoelastic material constant	$\beta'_{ab}$	stress-temperature coefficients
$\sigma_{ab}$	mechanical stress tensor	$\nu_0$	retardation time for Kelvin-Voigt model
$E_{ab}$	Maxwell's electromagnetic stress tensor	$\Omega$	uniform angular velocity
$k_{ab}$	heat conductivity coefficients	$\Psi_f, \delta_f, \bar{h},$	suitably prescribed functions
$\bar{t}_a = \sigma_{ab}n_b,$	tractions	$k_{ab}^{I*}$	additional material constant for GN theories
$\tau_1$	relaxation time	$T_0$	reference number

## References

- [1] M. Biot, "Thermoelasticity and irreversible thermo-dynamics," *J. Appl. Phys.*, vol. 27, pp. 249-253, 1956.
- [2] H.W. Lord and Y. Shulman, "A generalized dynamical theory of thermoelasticity," *J. Mech. Phys. Solids*, vol. 15, pp. 299-309, 1967.
- [3] A. E. Green and K. A. Lindsay, "Thermoelasticity," *J. Elast.*, vol. 2, pp. 1-7, 1972.
- [4] A. E. Green and P. M. Naghdi, "On undamped heat waves in an elastic solid," *J. Therm. Stresses*, vol. 15, pp. 252-264, 1992.
- [5] A. E. Green and P. M. Naghdi, "Thermoelasticity without energy dissipation," *J. Elast.*, vol. 31, pp. 189-208, 1993.
- [6] A. Berezovski, G.A. Maugin, "simulation of thermoelastic wave propagation by means of a composite wave-propagation algorithm," *J. Comput. Phys.* vol. 168, pp. 249-264, 2001.
- [7] S. C. Misra, S. C. Samanta and A. K. Chakrabarti, "Transient magnetothermoelastic waves in a viscoelastic half-space produced by ramp-type heating of its surface," *Comput.Struct.*, vol.43, pp. 951-957, 1992.
- [8] A. M. El-Naggar, A. M. Abd-Alla, M. A. Fahmy and S. M. Ahmed, "Thermal stresses in a rotating non-homogeneous orthotropic hollow cylinder," *Heat Mass Transfer*, vol. 39, pp. 41-46, 2002
- [9] A. M. El-Naggar, A. M. Abd-Alla, and M. A. Fahmy, "The propagation of thermal stresses in an infinite elastic slab," *Appl. Math.Comput.*, vol. 157, pp. 307-312, 2004.
- [10] A. M. Abd-Alla, A. M. El-Naggar and M. A. Fahmy, "Magneto-thermoelastic problem in non-homogeneous isotropic cylinder," *Heat Mass Transfer*, vol. 39, pp. 625-629, 2003.
- [11] A. M. Abd-Alla, M. A. Fahmy, and T. M. El-Shahat, "Magneto-thermo-elastic stresses in inhomogeneous anisotropic solid in the presence of body force," *Far East J. Appl. Math.*, vol. 27, pp. 499-516, 2007
- [12] A. M. Abd-Alla, M. A. Fahmy, and T. M. El-Shahat, "Magneto-thermo-elastic problem of a rotating non-homogeneous anisotropic solid cylinder," *Arch. Appl. Mech.*, vol. 78, pp. 135-148, 2008.
- [13] M. A. Fahmy, "Effect of initial stress and inhomogeneity on magneto-thermo-elastic stresses in a rotating anisotropic solid," *JP J. Heat Mass Transfer*, vol. 1, pp. 93-112, 2007.
- [14] M. A. Fahmy, "Thermoelastic stresses in a rotating non-homogeneous anisotropic body," *Numerical Heat Transfer. Part A: Applications*, vol. 53, pp. 1001-1011, 2008.
- [15] M. A. Fahmy, "Transient magneto-thermo-visco-elastic stresses in a rotating non-homogeneous anisotropic solid with and without moving heat source," *J. Eng. Phys. Thermophys.*, vol. 85, pp. 874-880, 2012.
- [16] M. A. Fahmy, "Finite difference algorithm for transient magneto-thermo-elastic stresses in a non-homogeneous solid cylinder," *Int. J. Mater. Eng. Technol.*, vol. 3, pp. 87-93, 2010.
- [17] M. A. Fahmy, "Influence of inhomogeneity and initial stress on the transient magneto-thermo-visco-elastic stress waves in an anisotropic solid," *World J. Mech.*, vol. 1, pp. 256-265, 2011.
- [18] M. A. Fahmy and T. M. El-Shahat, "The effect of initial stress and inhomogeneity on the thermoelastic stresses in a rotating anisotropic solid," *Arch. Appl. Mech.*, vol. 78, pp. 431-442, 2008.
- [19] H. Yan, Y. Liu, "An efficient high-order boundary element method for nonlinear wave-wave and wave-body interactions," *J. Comput.Phys.* vol. 230, pp. 402-424, 2011.
- [20] M. Shariyat, S. M. H. Lavasani, M. Khaghani, "Nonlinear transient thermal stress and elastic wave propagation analyses of thick temperature-dependent FGM cylinders, using a second-order point-collocation method," *Appl. Math. Modell.*, vol. 34, pp. 898-918, 2010.
- [21] A. M. Afsar and J. Go, "Finite element analysis of thermoelastic field in a rotating FGM circular disk," *Appl. Math. Modell.*, vol. 34, pp. 3309-3320, 2010.
- [22] G. M. Zhang and R. C. Batra, "Wave propagation in functionally graded materials by modified smoothed particle hydrodynamics (MSPH) method," *J. Comput. Phys.*, vol. 222, pp. 374-390, 2007.
- [23] A. G. Arani, R. Kolahchi, A. A. M. Barzoki and A. Loghman, "Electro-thermo-mechanical behaviors of FGPM spheres using analytical method and ANSYS software," *Appl. Math. Modell.*, vol. 36, pp. 139-157, 2012.
- [24] A. Khosravifard, M.R. Hematiyan and L. Marin, "Nonlinear transient heat conduction analysis of functionally graded materials in the presence of heat sources using an improved meshless radial point interpolation method," *Appl. Math.Modell.*, vol. 35, pp. 4157-4174, 2011.
- [25] T. Rangelov, Y. Stoyanov and P. Dineva, "Dynamic fracture behavior of functionally graded magnetoelectroelastic solids by BIEM," *Int. J. Solids Struct.*, vol. 48, pp. 2987-2999, 2011.
- [26] F. X. Zhou, S. R. Li and Y. M. Lai, "Three-dimensional analysis for transient coupled thermoelastic response of a functionally graded rectangular plate," *J. Sound Vib.*, vol. 330, pp. 3990-4001, 2011.

- [27] M. A. Fahmy, "A three-dimensional generalized magneto-thermo-viscoelastic problem of a rotating functionally graded anisotropic solids with and without energy dissipation," *Numer. Heat Transfer, Part A: Applications*, vol. 63, pp. 713-733, 2013.
- [28] M. A. Fahmy, "Generalized magneto-thermo-viscoelastic problems of rotating functionally graded anisotropic plates by the dual reciprocity boundary element method," *J. Therm. Stresses*, vol. 36, pp. 1-20, 2013.
- [29] D. Nardini and C. A. Brebbia, "A New approach to Free Vibration Analysis Using Boundary Elements," *Proceedings 4th International Conference on Boundary Element Methods*, Springer, 1982, pp. 312-326.
- [30] C. A. Brebbia, J. C. F. Telles and L. Wrobel, "Boundary element techniques in Engineering," New York: Springer-Verlag, 1984.
- [31] L. C. Wrobel and C. A. Brebbia, "The dual reciprocity boundary element formulation for nonlinear diffusion problems," *Comput. Methods Appl. Mech. Eng.*, vol. 65, pp. 147-164, 1987.
- [32] P. W. Partridge, C. A. Brebbia and L. C. Wrobel, "The dual reciprocity boundary element method," Southampton: Computational Mechanics Publications, 1992.
- [33] P. W. Partridge and L. C. Wrobel, "The dual reciprocity boundary element method for spontaneous ignition," *Int. J. Numer. Methods Eng.*, vol. 30, pp. 953-963, 1990.
- [34] M. A. Fahmy, "Implicit-explicit time integration DRBEM for generalized magneto-thermoelasticity problems of rotating anisotropic viscoelastic functionally graded solids," *Eng. Anal. Boundary Elem.*, vol. 37, pp. 107-115, 2013.
- [35] M. A. Fahmy, "Application of DRBEM to non-steady state heat conduction in non-homogeneous anisotropic media under various boundary elements," *Far East J. Appl. Math.*, vol. 43, pp. 83-93, 2010.
- [36] M. A. Fahmy, "A time-stepping DRBEM for magneto-thermo-viscoelastic interactions in a rotating nonhomogeneous anisotropic solid," *Int. J. Appl. Mech.*, vol. 3, pp. 1-24, 2011.
- [37] M. A. Fahmy, "Numerical modeling of transient magneto-thermo-viscoelastic waves in a rotating nonhomogeneous anisotropic solid under initial stress," *Int. J. Model. Simul. Sci. Comput.*, vol. 3, pp. 125002, 2012.
- [38] M. A. Fahmy, "Transient magneto-thermo-elastic stresses in an anisotropic viscoelastic solid with and without moving heat source," *Numer. Heat Transfer, Part A: Applications*, vol. 61, pp. 547-564, 2012.
- [39] M. A. Fahmy, "The effect of rotation and inhomogeneity on the transient magneto-thermo-visco-elastic stresses in an anisotropic solid," *ASME J. Appl. Mech.*, vol. 79, pp. 051015, 2012.
- [40] M. A. Fahmy, "A time-stepping DRBEM for the transient magneto-thermo-visco-elastic stresses in a rotating non-homogeneous anisotropic solid," *Eng. Anal. Boundary Elem.*, vol. 36, pp. 335-345, 2012.
- [41] M. A. Fahmy, "Transient magneto-thermoviscoelastic plane waves in a non-homogeneous anisotropic thick strip subjected to a moving heat source," *Appl. Math. Modell.*, vol. 36, pp. 4565-4578, 2012.
- [42] L. Gaul, M. Kögl and M. Wagner, "Boundary element methods for engineers and scientists," Berlin: Springer-Verlag, 2003.
- [43] C. Farhat, K. C. Park and Y. Dubois-Pelerin, "An unconditionally stable staggered algorithm for transient finite element analysis of coupled thermoelastic problems," *Computer Methods in Applied Mechanics and Engineering*, vol. 85, pp. 349-365, 1991.
- [44] J. Sladek, V. Sladek, P. Sulek, and Ch. Zhang, "Fracture analysis in continuously nonhomogeneous magneto-electro-elastic solids under a thermal load by the MLPG," *Int. J. Solids Struct.*, vol. 47, pp. 1381-1391, 2010.
- [45] M. A. Fahmy, "Thermal stresses in a spherical shell under three thermoelastic models using FDM," *Int. J. Numer. Methods Appl.*, vol. 2, pp. 123-128, 2009.